Ahmad et al., J Material Sci Eng 2016, 5:6
DOI: 10.4172/2169-0022.1000289

Journal of Material Sciences & Engineering

Research Article Open Access

Attenuation Performance of Polymer Composites Incorporating NZF Filler for Electromagnetic Interference Shielding at Microwave Frequencies

Ahmad AF[1]*, Abbas Z[2], Obaiys SJ[3] and Abdalhadi DM[2]

[1]*Materials Processing and Technology Laboratory, Institute for Advance Material, Universiti Putra Malaysia, Serdang, Selangor Darul Ehsan, Malaysia*
[2]*Department of Physics, Faculty of Science, Universiti Putra Malaysia, Serdang, Selangor Darul Ehsan, Malaysia*
[3]*School of Mathematical and Computer Sciences, Heriot-Watt University Malaysia, Putrajaya, Malaysia*

Abstract

Polymer composites have been thoroughly explored for future electromagnetic interference (EMI) applications owing to their unique combination of electrical, mechanical, and optical properties. The composition, morphology, and surface characteristics of the filler material play critical roles in regulating the composite activity. We studied the formation, synthesis and EM attenuation properties of nickel zinc ferrite (NZF) + Polycaprolactone (PCL) micro-composites that were prepared via the conventional mixed oxide (CMO) technique. Compared with other preparation routes, CMO may provide the advantages of a simple process and the ability for mass production and controlled product formation. A rectangular waveguide connected to a vector network analyser coaxial cable was employed to measure the scattering parameters [S] for use in determining the attenuation values of NZF+PCL substrates for a variety of NZF% values. Measurement tests showed a simultaneous increment in the attenuation value with the filler percentage. NZF+PCL samples of 1-mm thickness were able to attenuate microwave frequencies by up to ~3.33 dB, where the highest attenuation magnitude of 8.599 dB over a large area was attributed to the 12.5% NZF filler content at 12 GHz. Thus, a low transmission of waves resulted from the high shielding effectiveness (SE) values that showed a maximum 6.86 dB EM interference. Scanning electron microscopy (SEM) was utilized to analyse the average particle size (1.45 μm) of the filler powder.

Keywords: Microwave; Rectangular waveguide; Composites; FTIR; SEM and T/R coefficients

Introduction

Different engineering applications require different minimum values of shielding effectiveness (SE), where the selection of the shielding materials is an important factor in their design. Knowledge of the behaviour of a material placed in an electromagnetic interference (EMI) field is of immense importance, particularly for military hardware, electronics, communication, and industrial applications and shielding [1,2]. It is vital to understand that the transmission coefficient measurements enable an attenuation analysis for materials of good microwave absorption. Attenuation is a function that can be affected by a group of factors. The SE of a material depends on both the conductivity and permittivity values, but for high-frequency shielding, the conductivity dominates. Materials with high conductivity values provide excellent SE results [3]. Commonly, a composite consists of filler and matrix, where the filler is usually surrounded by matrix materials to keep the resulting composite in position. Matrix materials must be flexible, lightweight, corrosion resistant, and of lower cost than metals. Polycaprolactone (PCL) is an excellent microwave-absorbing material and well known as a material for EMI SE in both near and far fields [4]. The enumerated characteristics such as the simplicity of fabrication, light weight, low cost, and excellent insulation properties play a major role in the design of advanced materials that are suitable for a variety of applications, such as electrodes, sensors and electrical devices of high frequency [5-7]. The properties of the polymer composites are affected by factors such as the inherent characteristics of each component, contact, dimension and shape of the fillers, and the nature of their interfaces [8]. Ferrites are very good dielectric materials whose main constituents are oxygen, iron and one or more metallic elements such as Ni and Zn that have many applications at microwave frequencies [9]. The properties of nickel zinc ferrite (NZF) composites can be tailored by controlling the preparation conditions and the amount of metal ion substitution. Their useful characteristic properties such as electrical resistivity, low dielectric loss, and chemical stability enable them to contribute in both the domestic and industrial sectors [10]. A composite of a ferrite material with a good polymer matrix will not only reduce the cost and enhance the structural properties of the outcomes but also increase the ability to control the EMI properties, particularly when operating at the high-frequency range [9,11]. Ferrite-polymer composites are widely studied due to their novel properties of simple preparation, light weight, low cost, better electronic properties, good optical properties, environmentally friendliness and high stability in air that make them highly suitable for many applications, such as EMI SE and microwave absorption [12].

Herein, the synthesis of (2.5%, 5%, 7.5%, 10%, and 12.5%) NZF+PCL substrate of 1mm thickness that show great EM propagation and affect the absorption properties at 8-12 GHz is achieved. The microwave properties of the samples were investigated using a rectangular waveguide connected with a vector network analyser coaxial cable. The total volume fraction of the composites was set to 15 g and divided into 1 g, 2 g, 3 g, 4 g and 5 g, with respect to the NZF%.

Experimental

Preparation of nickel zinc-ferrite composites

In this work, the formation of Ni-Zn-ferrite material was carried

***Corresponding author:** Ahmad AF, Materials Processing and Technology Laboratory, Institute for Advance Material, Universiti Putra Malaysia, Serdang, Selangor Darul Ehsan, Malaysia, Tel: 60173370907; E-mail:ahmad_al67@yahoo.com

Received September 28, 2016; **Accepted** October 15, 2016; **Published** October 25, 2016

Citation: Ahmad AF, Abbas Z, Obaiys SJ, Abdalhadi DM (2016) Attenuation Performance of Polymer Composites Incorporating NZF Filler for Electromagnetic Interference Shielding at Microwave Frequencies. J Material Sci Eng 5: 289. doi:10.4172/2169-0022.1000289

out using the conventional mixed oxide (CMO) method, which is a highly favoured route in commercial ferrite production due to its relative simplicity, scalability, high mass production and economic efficiency. The oxide raw materials of NiO (99.7% purity), ZnO (99.9% purity) and Fe_2O_3 (99.7% purity) were mingled well together and then weighed according to the zinc ferrite (Ni_x Zn_{1-x} Fe_2O_4) stoichiometric equation [13].

$$xNiO+(1-x)ZnO+Fe_2O_3 \rightarrow Ni_xZn_{1-x}Fe_2O_4 \quad (1)$$

The mixture was then carefully ground in a ball mill and exposed to heat to ensure the particle homogeneity of the powder. After that, the milled powder was moulded and pressed into the required shape for the final sintering process of 900-1000°C for 10 hours to obtain the crystalline structure of the materials under test.

Preparation of NZF+PCL composites

The NZF+PCL composites were prepared by the melt blending technique using a Thermo Haake Poly Drive extruder with a three-phase motor with a drive of 1.5 kW, 3 × 230 V, 40 A and speed range of 0-120 rpm. The resulting crude blends have to undergo hot-pressing to prepare a thin film for each blend. Compounding samples of 15 g each were prepared with different percentages of NZF and PCL with a rotation speed of 50 rotations per minute (rpm). The NZF+PCL composites were preheated for 10 minutes with upper and lower platen temperatures of 80°C, which is close to the PCL melting point (60-70°C). A venting time of 10 seconds was allowed to release the bubbles and reduce the voids, and the samples were then pressed at the same temperature for another 10 minutes. Finally, a cooling pressing of 110 kg/cm^2 was carried out for another 10 minutes at 25°C for the best substrate fabrication result. Figure 1 shows the prepared NZF+PCL substrates, and Table 1 presents the different compositions that were utilized in the experimental step.

Preparation of substrates

The samples were carefully fabricated to fit the rectangular waveguide dimensions best and to prevent any scratch or crack that may alter the measurement results. The substrates were prepared by placing 10 g of the blends into a mould of 8-10 cm^2 dimensions and 1 mm thickness. The samples were then restricted to suit the internal waveguide dimensions perfectly and remove any possibility of an air gap around the sample walls. A vector network analyser (VNA) (Agilent 8750B) based waveguide measurement technique was utilized to measure the S-parameters of the two-port network formed by placing the substrate inside the rectangular waveguide. The material properties were studied in the X-band (8-12GHz) regions of the microwave frequency spectra. Figure 2 shows the experimental technique of this work.

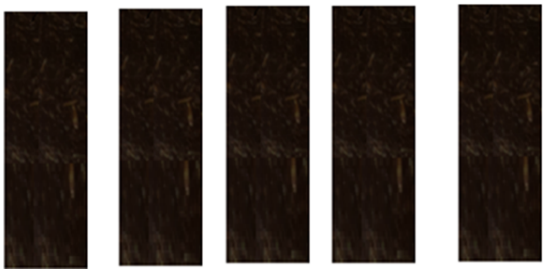

Figure 1: Prepared substrate of NZF+PCL micro-composites.

NZF%	PCL %
2.5	97.5
5	95
7.5	92.5
10	90
12.5	87.5

Table 1: Percentages of NZF and PCL in the prepared composites.

Figure 2: A rectangular waveguide connected to a VNA for the measurement set up.

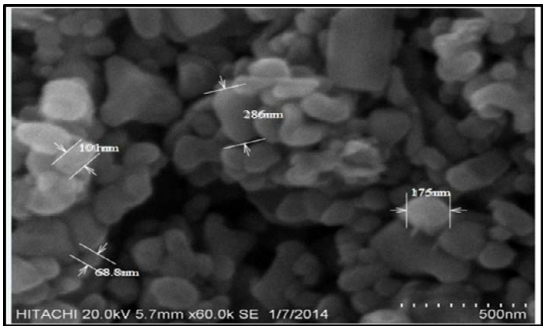

Figure 3: SEM micrograph of $N_{0.5}Z_{0.5}$ Fe_2O_4 micro-particles prepared via CMO technique.

Results and Discussion

Morphological properties of NZF micro-particles

The prepared NZF fillers were analysed using scanning electron microscopy (SEM) (S-3400N) with a field emission gun and an accelerating voltage of 10 kV. A careful observation of the SEM image presented in Figure 3, focusing on the variety of signals, reveals a good arrangement of particles. The spherical structure of the synthesized NZF particles shows an average size of approximately 69 to 286 mm, which confirms the successful preparation.

Measurement of the scattering parameters [S]

It is known that the EM properties can be calculated from the scattering parameters [S]. The boundaries of the materials under test (MUT) are defined, and the reflection coefficients (S_{11}) and transmission coefficients (S_{21}) can then be measured accurately [14]. In the transmission/reflection (T/R) method of a waveguide, the samples were inserted in a piece of transmission line, and the properties of the material were deduced based on the rejection of the material and the transmission through the material [15]. This method is commonly performed in the measurement of the EMI properties of materials

due to the field-focusing ability of the microwave guides that enables accurate measurements at microwave frequencies, where the EM waves propagate through the microwave guides at 8-12 GHz [16].

The measurement was performed at the connectors of the waveguides. However, the specimen was considered as a two-port network whose S_{11} and S_{21} values used a "thru reflect line" (TRL) calibration that needs to be performed to set the planes of the incident and reflected waves at the ends of the waveguides rather than that at the connectors [17]. After the calibration step, the accuracy of the calibration technique was evaluated by measuring the [S] of air (without sample) and Teflon (PTFE) samples. Figure 4 presents the [S] curves of the standard materials, where the values of $|S_{21}|$ were higher than those of $|S_{11}|$. Theoretically, the value of $|S_{21}|$ should be close to unity.

The responses of a network to external circuits can also be described by the input and output waves. The input [a] and output [b] waves at port 1 and port 2 are denoted as a_1, a_2, b_1 and b_2, respectively. These parameters (a_1, a_2, b_1, and b_2) may be voltage or current, and in most cases, we do not distinguish between whether they are voltage or current [11]. The relationships between [a] and [b] are often described by [S] values, Where,

$$[b]=\begin{bmatrix} S_{11} & S_{12} \\ S_{21} & S_{22} \end{bmatrix}\begin{bmatrix} a_{11} & a_{12} \\ a_{21} & a_{22} \end{bmatrix}; \quad or \quad [b]=[S][a] \tag{2}$$

It is known that the S_{11} and S_{21} parameters can be measured directly at microwave frequencies. Generally, the complex form of [S] can be defined as

$$\left.\begin{aligned} S_{qq} &= \frac{b_q}{a_q}\ (q=1,2) \\ S_{pq} &= \frac{b_p}{a_p}\ (p\neq q;\ p=1,2;\ q=1,2) \end{aligned}\right\} \tag{3}$$

Then, the S_{11} values are defined as

$$\Gamma_q = S_{qq} = \frac{b_q}{a_q} \tag{4}$$

The S_{21} values are defined by

$$T_{q\to p} = S_{qq} = \frac{b_p}{a_p} \tag{5}$$

[S] can then be obtained by the combinations of these four waves according to Eq. (3), where the parameters a_1, a_2, b_1, and b_2 are normally used to measure the corresponding four waves. The signal separation devices ensure that the four waves are measured independently [11]. The obtained VNA results of S_{21} were then used to compute the attenuation results of the MUT by the following equation:

$$Attenuation\,(dB) = -20\log(S_{21}) \tag{6}$$

It is known that several actions such as transmission, reflection and absorption are performed as EM radiation falls on a shielding material [18]. The total EMI SE (SE_T) is defined as the summation of all of the contributors to the SE (absorption loss (SE_A), reflection loss (SE_R), and multiple reflection loss (SE_M)):

$$SE_T = SE_A(dB) + SE_R(dB) + SE_M(dB) \tag{7}$$

For a single layer of shielding material, when SE_A is ≥10 dB, then $SE_M = 0$, so it can be ignored [18]. Thus, the SE_T in Eq. (7) can be written as

$$SE_T = SE_A(dB) + SE_R(dB) \tag{8}$$

The incident EM wave power inside the shielding material can be estimated as

$$SE_R = -10\log(1-R) \tag{9}$$

$$SE_R = -10\log\left(\frac{T}{1-R}\right) \tag{10}$$

where the transmittance (T) value is equal to $(S_{21})^2$, and the reflectance (R) is $(S_{11})^2$.

While the basic mean-value ($\bar{x}$) analysis of attenuation, SE_R, SE_A and SE_T values for different percentages of NZF+PCL composites based excel program is calculated by

$$\bar{x} = \frac{\sum_{i=1}^{n} x_i}{n}; \qquad n = 200 \tag{11}$$

Figures 5 and 6 show proportional graphs of the measured $|S_{11}|$

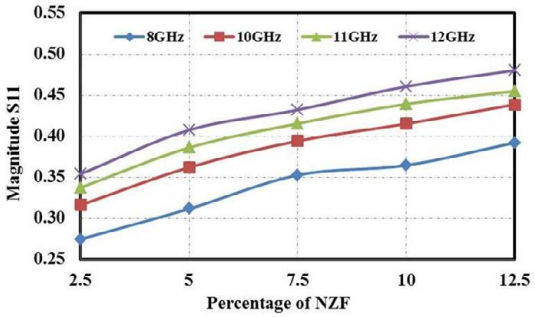

Figure 5: Percentage of NZF filler content vs transmission coefficient values in the microwave frequency range.

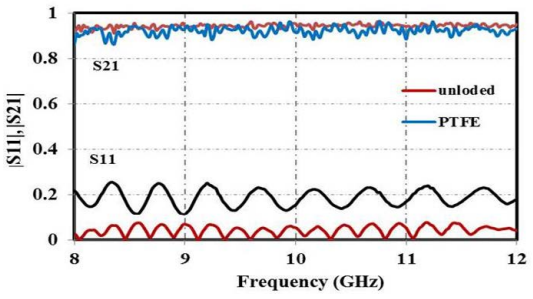

Figure 4: Measured $|S_{11}|$ and $|S_{21}|$ of air and PTFE at microwave frequencies (8-12 GHz).

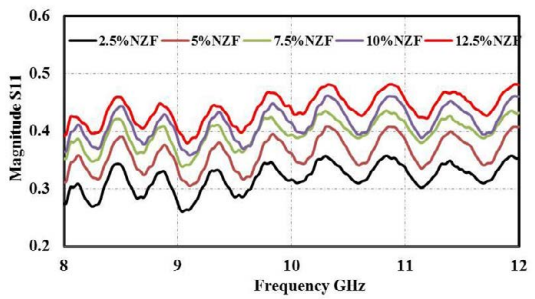

Figure 6: Measured $|S_{11}|$ in the microwave frequency range for all samples.

values with the NZF micro-filler percentage and the frequency, respectively. The highest $|S_{11}|$ value of ~0.48 was recorded for the highest NZF% of 12.5 and the maximum frequency of 12 GHz for all samples under test.

Oppositely, Figures 7 and 8 shows an inversely proportional relationship between the filler composition and frequency range and the $|S_{21}|$ values, where increases in the filler content and frequency range both reduce the $|S_{21}|$ values. These results demonstrate the impedance mismatch theory, where materials with a higher permittivity exhibit lower transmission coefficient values [19]. This might be attributed to the perfect dispersion of the filler in the matrix, as the homogeneity of the particle dispersion in the matrix will tend to increase or decrease the transmission of the EM radiation depending on the dispersion of the NZF particles in the matrix.

To calculate the attenuation of the various NZF+PCL micro-composites, all the obtained $|S_{21}|$ results were input into Eq. 6. The calculated results, as shown in Figure 9, confirm the proportional relationship between the attenuation outcomes of the NZF+PCL micro-composites and the filler composition. From Figure 9, it can be clearly observed that the lowest attenuation value was calculated for the 2.5% NZF micro-particle filler, whereas the highest attenuation result was observed for the 12.5% NZF micro-particle filler.

Further analysis is provided in a graph of the filler content against the attenuation values that is presented in Figure 10. The highest attenuation value (~8.6 dB) was obtained from the highest filler content (12.5%). Thus, a reduction in the $|S_{21}|$ values was clearly observed for the higher valves of NZF-filler content, as depicted in Figure 7. Based on the above, Table 2 provides a tabulated summary of the mean attenuation values, highlighting the proportional relationship between the attenuation magnitude and NZF filler composition.

The exact statistical algorithm based $\bar{x}$ analysis has provided efficient results that allow us to properly analyze the different percentages of NZF+PCL composites. Figure 11 shows a graph of the mean attenuation values of the NZF+PCL micro-composites against the filler content. The attenuation values constantly increased with the NZF filler content.

EMI SE application

Figure 12 shows the variation in the SE_T values due to the alteration of the NZF loading, SE_R and SE_A of the NZF+PCL at 8-12 GHz. The

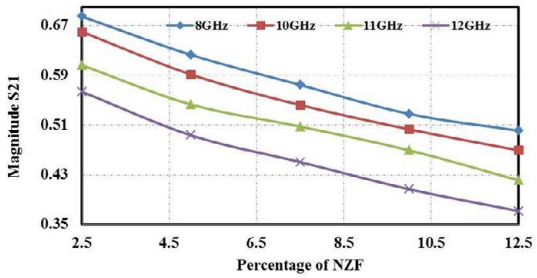

Figure 7: Percentage of NZF filler content vs measured $|S_{21}|$ values at 8-12 GHz.

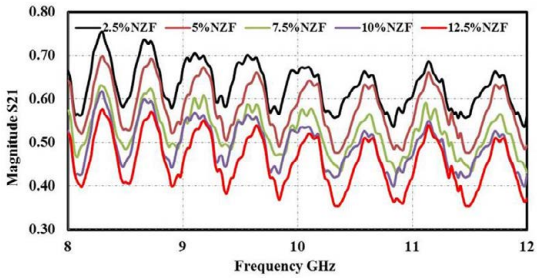

Figure 8: Measured $|S_{11}|$ values for all samples at the X-band frequency.

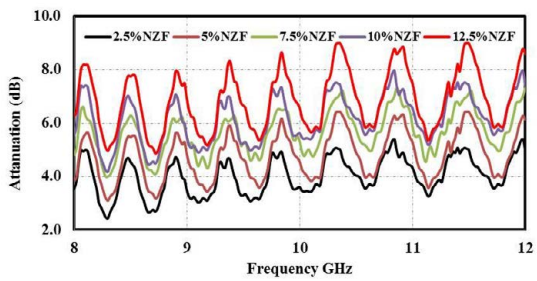

Figure 9: Calculated attenuation results of different NZF+PCL compositions at 8-12 GHz.

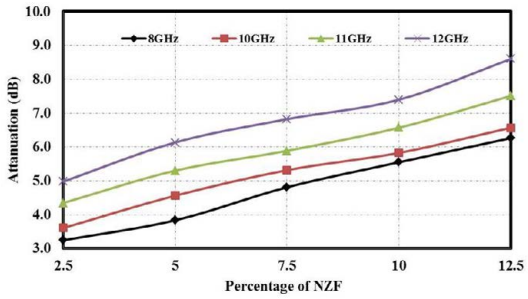

Figure 10: Percentage NZF filler contents vs attenuation in the selected frequency range.

NZF%	8 GHz	10 GHz	11 GHz	12 GHz
2.5	3.245	3.607	4.346	4.978
5	3.835	4.562	5.301	6.133
7.5	4.811	5.316	5.889	6.822
10	5.549	5.827	6.57	7.396
12.5	6.263	6.569	7.511	8.599

Table 2: Mean values of attenuation for different percentages of NZF+PCL micro-composites at microwave frequencies.

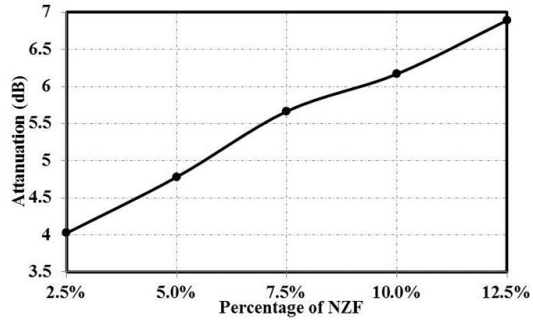

Figure 11: Mean attenuation of NZF+PCL micro-composites vs NZF-filler content.

difference between SE_A and SE_R increases with the NZF content, suggesting that the absorption contribution to the EM SE increases with the NZF loading increment. The primary mechanism of the EMI shielding is usually a reflection of the EM radiation incident on the shield, which is a consequence of the interaction of the EMI radiation with the free electrons on the surface of the shield. Absorption is usually a secondary mechanism of EMI SE, whereby electric dipoles in the shield interact with the EM waves in the radiation [11,18]. Another reason for such a variation between the SE_R and SE_A values may be the interfacial polarization of the PCL by the NZF, which increases the absorption component. The values of SE_A increase from ~ 2.78 dB at 2.5% to ~6.86 dB at 12.5% loading. Based on the above, the EMI SE results are mostly independent of the frequency in the X-band.

From Figure 13, the EMI SE value increased dramatically with a slight NZF vol. % increment. In fact, the highest EMI SE of approximately 6.86 dB was achieved from 12.5% NZF in the composite at a particular frequency in the X-band region. Moreover, it was found that SE_A increases much faster than SE_R as the NZF content increments.

NZF+PCL composites can be used for many shielding applications by adjusting the filler content [9]. For example, an addition of only 2.5% NZF filler in the NZF+PCL composite already satisfies the minimum 3.339 dB SE requirement for the aircraft structural shielding of an antenna based on Wireless Avionics Intra-Communications specifications [20]. However, the scope of this paper is to determine the minimum percentage of filler for a sample of 1 mm thickness to obtain a maximum 6.86 dB SE. The mean values of SE_R, SE_A and SE_T for the composites which calculated by $\overline{x}$ in Eq. 11 for different NZF% are listed in Table 3 below, where the widely used $\overline{x}$ statistical analysis are reasonably accurate.

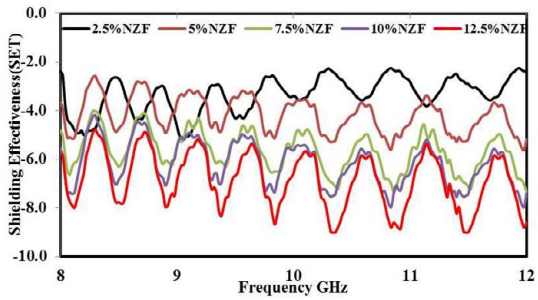

Figure 12: SE_T as a function of frequency measured in the 8-12 GHz range of different NZF+PCL composites.

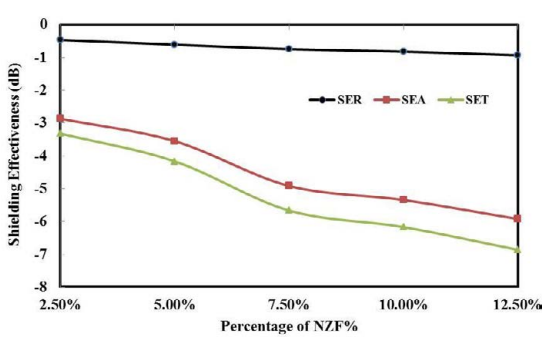

Figure 13: Comparison of SE_T, SE_R, and SE_A in the 8–12 GHz range for NZF+PCL composites.

NZF%	SE_R(dB)	SE_A(dB)	SE_T(dB)
2.5	-0.469	-2.87	-3.339
5	-0.613	-3.556	-4.169
7.5	-0.749	-4.917	-5.665
10	-0.824	-5.344	-6.168
12.5	-0.937	-5.923	-6.86

Table 3: Mean SE_R, SE_A and SE_T of NZF + PCL composites.

Conclusions

The shielding effectiveness is defined as the process of using specialized materials to reduce the EMI fields or waves that enter a specific enclosure. The shielding performance highly depends on type, size and thickness of the utilized materials along with the frequency range. In this work, NZF+PCL micro-composite structures have been successfully synthesized for potential SE and absorption applications. The EM propagation and attenuation properties of these composites in waveguides were theoretically and experimentally investigated in the 8-12 GHz range of frequency. For microwave characterization, the effects of various NZF compositions on the attenuation of the NZF+PCL composites were calculated using the measured $|S_{21}|$ result based rectangular waveguide technique and were implemented in shielding effectiveness and absorption applications. The attenuation of the different NZF+PCL micro-composites showed that the attenuation magnitude increased with the filler content, which confirmed the correlation between the attenuation value and the NZF-filler content.

Acknowledgements

The authors sincerely extend their gratitude to Universiti Putra Malaysia for providing financial support and facilities for the completion of this work.

References

1. Canan D, Papila M (2010) Dielectric behavior characterization of a fibrous-ZnO/PVDF nanocomposite. Polym Composite 31: 1003-1010.
2. Xiaogu H, Zhang J, Lai M, Sang T (2015) Preparation and microwave absorption mechanisms of the Ni-Zn ferrite nanofibers. J Alloy Compd 627: 367-373.
3. Ahmad AF, Abbas Z, Obaiys SJ, Ibrahim NA, Zainuddin MF (2015) Microwave characterization of bio-composites materials based finite element and nicholson–ross–weir methods. Malaysian Journal of Science 34: 180-184.
4. Geetha S, Satheesh Kumar KK, Rao CRK, Vijayan M, Trivedi DC (2009) EMI shielding: methods and materials—A review. J Appl Polym Sci 112: 2073-2086.
5. Ahmad FA, Abbas Z, Obaiys SJ, Ibrahim N, Hashim M, et al. (2015) Theoretical and numerical approaches for determining the reflection and transmission coefficients of OPEFB-PCL composites at X-band frequencies. PloS one 10: e0140505.
6. Elammaran J, Hamdan S, Rahman MR, Bin Bakri MK (2014) Comparative study of dielectric properties of hybrid natural fiber composites. Procedia Engineering 97: 536-544.
7. Harun B (2011) Complex permittivity, complex permeability and microwave absorption properties of ferrite–paraffin polymer composites. J Magn Magn Mater 323: 1882-1885.
8. Roman K (2012) Thermal and electrical properties of nanocomposites, including material properties. TU Delft, Delft University of Technology.
9. Ahmad AF, Zulkifly A, Obaiys SJ, Ibrahim NA, Hashim M, et al. (2016) Permittivity properties of nickel zinc ferrite-oil palm empty fruit bunch-polycaprolactone composite. Procedia Chemistry 19: 603-610.
10. Khoon TF, Hassan J, Mokhtar N, Hashim M, Ibrahim NA (2011) Dielectric behavior of $Ni_{0.1}Zn_{0.9}Fe_2O_4$-polypropylene composites at low microwave frequencies. Solid State Science and Technology 19: 207-213.
11. Fahad A, Abbas Z, Obaiys SJ, Ibrahim N, Yakubu A (2016) Dielectric behavior of OPEFB reinforced polycaprolactone composites at X-band frequency. Int Polym Proc 31: 18-25.
12. Liangchao L, Liu H, Wang Y, Jiang J, Xu F (2008) Preparation and magnetic

properties of Zn Cu Cr La ferrite and its nanocomposites with polyaniline. J Colloid Interf Sci 321: 265-271.

13. Cedomir J, Nikolic AS, Gruden-Pavlovic M, Pavlovic MB (2012) Mechano–chemical synthesis of stoichiometric nickel and nickel–zinc ferrite powders with Nicolson–Ross analysis of the absorption coefficients. J Serb Chem Soc 77: 497-505.
14. Paula D, Luiz A, Rezende MC, Barroso JJ (2011) Experimental measurements and numerical simulation of permittivity and permeability of teflon in X band. Journal of Aerospace Technology and Management 3: 59-64.
15. Harun B (2012) Electromagnetic propagation and absorbing property of ferrite-polymer nanocomposite structure. Progress in Electromagnetics Research M 25: 269-281.
16. Bayrakdar H (2011) Magnetically modified biocells in constant magnetic field. J Magn Mater 323: 1882-1885.
17. Doug R (2008) ARFTG 50 year network analyzer history.
18. Xingcun Colin T (2016) Advanced materials and design for electromagnetic interference shielding. CRC Press.
19. Pozar DM (2009) Microwave engineering. John Wiley and Sons, USA.
20. WAIC (2012) Agenda Item 1.17 update and status on implementing of a regulatory framework for WAIC. Presentation for ICAO Regional Meeting, Lima, Peru.